Reliability Prediction of Integrated LED Lamps with Electrolytic Capacitor-Less LED Drivers

Sun, B; Fan, Xuejun; van Driel, Willem Dirk ; Zhang, Guo Qi

DOI
10.1007/978-3-319-58175-0_16

Publication date
2018

Document Version
Final published version

Published in
Solid State Lighting Reliability Part 2

Citation (APA)
Sun, B., Fan, X., van Driel, W. D. (Ed.), & Zhang, G. Q. (2018). Reliability Prediction of Integrated LED Lamps with Electrolytic Capacitor-Less LED Drivers. In W. D. van Driel, X. Fan, & G. Q. Zhang (Eds.), *Solid State Lighting Reliability Part 2: Components to Systems* (1 ed., pp. 455-486). (Solid State Lighting Technology and Application Series; Vol. 3). Springer. https://doi.org/10.1007/978-3-319-58175-0_16

Chapter 16
Reliability Prediction of Integrated LED Lamps with Electrolytic Capacitor-Less LED Drivers

B. Sun, Xuejun Fan, Willem Dirk van Driel, and Guo Qi Zhang

Abstract This chapter investigates the reliability of the integrated LED lamps with electrolytic capacitor-less LED drivers. Firstly, the impact of the interaction between the degradations of the LED light source and the driver on the lumen depreciation is studied. The electronic-thermal simulation was carried out to obtain the history of temperatures of LED and driver, the driver's output current, and the luminous flux considering the variations of temperature and current throughout the operation life. It is found that the ultimate lamp's lifetime is significantly less than the individual lifetimes of the preselected LED and driver. It is concluded that it is necessary to apply the electronic-thermal simulations to predict the lifetime of LED lamps when driver's lifetime is comparable to the LED's lifetime. Secondly, this chapter focuses on predicting the catastrophic failure of an electrolytic capacitor-free LED driver during the lumen depreciation process. Electronic-thermal simulations are utilized to obtain the lamp's dynamic history of temperature and

B. Sun (✉)
Beijing Research Center, Delft University of Technology, No.A35, Qinghua East Road, Beijing 100083, China
e-mail: sandysun23@gmail.com

X. Fan
State Key Laboratory of Solid State Lighting (Changzhou Base), Changzhou, China

Department of Mechanical Engineering, Lamar University, Beaumont, USA
e-mail: xuejun.fan@lamar.edu

W.D. van Driel (✉)
Philips Lighting, High Tech Campus, Eindhoven, The Netherlands

Delft University of Technology, EEMCS Faculty, Delft, The Netherlands
e-mail: willem.van.driel@philips.com

G.Q. Zhang
State Key Laboratory of Solid State Lighting, Institute of Semiconductors, Chinese Academy of Sciences, Beijing, China

State Key Laboratory of Solid State Lighting (Changzhou Base), Changzhou, China

EEMCS Faculty, Delft University of Technology, Delft, The Netherlands
e-mail: g.q.zhang@tudelft.nl

W.D. van Driel et al. (eds.), *Solid State Lighting Reliability Part 2*, Solid State Lighting Technology and Application Series 3, DOI 10.1007/978-3-319-58175-0_16

electrical current for two distinct modes: constant current mode (CCM) and the constant optical output (CLO) mode, respectively. A fault tree method is applied to calculate the system's MTTF, and the LED's lifetime also is calculated. The CLO mode increases the LED's current exponentially to maintain the constant light output. As a result, junction temperatures of LEDs, MOSFET, and diode rise significantly, leading a shorter lifetime and MTTF. Compare with the current of the MOSFET, the increased junction temperature has larger effects on the failure rate. The MOSFET contributes more to the driver's failure rate than the diode. For the CCM mode, junction temperatures increase slightly and have a little shorter lifetime and MTTF.

16.1 Introduction

Light-emitting diode (LED) has been regarded as one of the most promising lighting solutions due to its energy efficiency, flexible controllability and long life flight source, a driver, control gears, secondary optical parts, and heat dissipation components. The LED light source often has a lifetime as long as 25,000–100,000 h [1, 2], but the LED driver has a shorter life than the light source, in particular, when electrolytic capacitors are utilized [3–5]. Many studies have focused on the degradation analysis of LED only, without taking consideration of the driver degradation [2, 6–10]. For example, an accelerated test method of luminous flux depreciation for LED lamps or luminaires has been developed to reduce the test time within 2000 h at an elevated temperature [2]. Degradations of LEDs in the high-temperature-humidity environment have been studied [6, 7]. The LED color shift caused by optical materials has been investigated [8, 9]. For the degradation of LED drivers, if the driver's lifetime is much shorter than LED's life, the degradation of LED light source may not be significant to the driver's lifetime. With such an assumption, a physics-of-failure (PoF)-based reliability prediction methodology for LED drivers has been developed to estimate the failure rate distribution of an electrolytic capacitor of the given LED driver systems [3].

Electrolytic capacitors are often used [11–18] in commercial LED drivers. In most of the single- and two-stage mainstream commercial LED drivers, electrolytic capacitors are used as energy storages and buffers [11, 12], including buck [14, 15], buck-boost [18], and fly-back drivers [13]. However, the electrolytic capacitor is considered as the weakest component in LED drivers [3–5]. Since electrolytic capacitor's lifetime is much less than that of LED's lifetime, the effect of LED's degradation may not be significant on its driver's reliability [3, 19]. A physics-of-failure (PoF)-based reliability prediction methodology for LED drivers has been developed by the authors to estimate the failure rate distribution of an electrolytic capacitor of the given LED driver systems [3]. In recent years, several electrolytic capacitor-less LED drivers have been presented to improve driver's lifetime, including buck-boost single-ended primary inductor converter (SEPIC) [20], valley-fill SEPIC driver [21], boost-fly-back driver [22] and SEPIC twin-bus buck driver [23]. Moreover, electrolytic capacitor eliminating circuits have also been installed into the mainstream LED drivers, such as power control (PC) converter

[24], two-phase dual asymmetrical half-bridge converter [25], bidirectional buck-boost converter [26], harmonic injection circuits [27], and LC filters [28, 29]. In addition, with the help of new technologies, for instance, resonance-assisted filter [14] and variable on-time control method [15], the lifetime of electrolytic capacitors can also be improved. For an electrolytic capacitor-less LED driver, the LED light source and the driver may have comparable lifetimes [30–32].

When the lifetime of the LED light source is much longer than the driver's, depreciation of the LED light source has little impact on the entire system during the process of the driver's failure. In the case that the LED light source and the driver have similar lifetimes, the lumen depreciation and the driver's failure coexist in the LED lamp and may interact with each other. The question arises that what is the interaction of two simultaneous failure modes: the LED depreciation and the driver's failure, during lamp operation? In this chapter, failures of the LED driver include the catastrophic failure and the degradation which leads to failures of entire system. Thus, there are two combinations: degradations of the LED light source and the driver and LED's depreciation and driver's catastrophic failure.

If degradations of the LED light source and the driver coexist, their interactions become significant factors in determining the lifetime of the LED lamp [33–37]. Both degradations are strongly affected by temperature and time. The LED light source degrades gradually over a long period, which is known as the lumen flux depreciation. During the degradation of the LED light source, its efficacy is reduced; thus, more heat dissipation is expected. On the other hand, when the driver degrades, the electrical current output to the LED light source will decrease over time. Such a process will affect the heat generations of both driver and LEDs. For an integrated lamp, where the LED light source and driver are assembled together, the heat generated by LEDs and the driver will determine the junction temperature of the LED light source as well as the driver's temperature. Such temperatures continuously change over time since LED heat dissipation depends on time, temperature, and current from the driver. In the meantime, the driver's performance also depends on time and temperature. Ultimately the LED's lumen flux depreciation is affected by the degradations of both LED drivers and LED light source. However, there is little systematic research on LED system reliability when LED's degradation and driver's failures coexist during operating conditions.

The catastrophic failure rate of an LED driver depends on its rate of the critical components, such as the MOSFETs and power diodes [34, 38]. The total rate of catastrophic failures determines the mean time to failure (MTTF) for the driver. At the same time, LED experiences degradation that is dependent on driver's output current, LED's junction temperature, and time. Generally, the lifetime of LED is given in terms of the expected operating hours until light output has depreciated to 70% of initial levels. In this sense, there are two distinct concepts of lifetimes involved in an LED system: mean time to failure (e.g., driver) and LED's lifetime in terms of luminous flux depreciation. When these two concepts are far different, it is obvious that they do not interact each other. Many commonly used reliability prediction methods consider the catastrophic failures at constant conditions without the interaction with LED degradation. Few systematic studies have been conducted to predict the reliability of the LED lamp when the MTTF is comparable to the LED's lifetime.

Intelligent driver and control techniques have been applied to LED systems. For instance, the constant light output (CLO) mode has been implemented in driver design to eliminate the lumen depreciation [39]. In contrast with the constant current mode (CCM), LED drivers in CLO mode usually have optical feedback functions and can adjust their output current to maintain the light output. It has claimed that such technology can eliminate the lumen depreciation during long-term operation. However, the system's reliability with constant light output technology has not yet been studied.

This chapter contains two major sections. In Sect. 16.2, an integrated LED lamp with an electrolytic capacitor-free driver is considered to study the coupling effects of both the LED light source and the driver's degradations on light output. The driver is assumed to have a comparable lifetime with the LED light source. The electronic-thermal simulation was carried out to obtain the history of temperatures of LED and driver, the driver's output current, and the luminous flux considering the variations of temperature and current throughout the operation life. Generally, the useful lifetime of LED lighting products is typically given in terms of the expected operating hours until light output has depreciated to 70% of initial levels [2]. Section 16.3 focuses on predicting the catastrophic failure of an electrolytic capacitor-free LED driver during the lumen depreciation process. The overall catastrophic failure rate of the critical components in this driver is considered as functions of temperature and current. Electronic-thermal simulations are utilized to obtain the lamp's dynamic history of temperature and electrical current for two distinct modes: constant current mode (CCM) and the constant optical output (CLO) mode, respectively. A fault tree method is applied to calculate the system's MTTF, and the LED's lifetime in terms of light output can also be calculated.

This chapter is organized as follows. Section 16.2 considers the coupling effects of degradations of the LED light source and the driver on system's lifetime. In Sect. 16.3, prediction on the catastrophic failure of LED driver during the lumen depreciation process is introduced. Section 16.4 concludes this chapter finally.

16.2 Coupling Effects of Degradations

This section studies the impact of the interaction between the degradations of the LED light source and the driver on the lumen depreciation. As using the electrolytic capacitor-free driver, the driver is assumed to have a comparable lifetime with the LED light source. In this case, degradations of the LED light source and the driver may coexist; their interactions become significant factors in determining the lifetime of the LED lamp [33–37].

The electronic-thermal simulation was carried out to obtain the history of temperatures of LED and driver, the driver's output current, and the luminous flux considering the variations of temperature and current throughout the operation life. Circuit simulations are carried out first to obtain the power distributions and output current and the voltage to LEDs. Thermal simulations are subsequently performed based on power distribution to obtain the temperature distributions of the LED lamp, in particular, LED junction temperature driver's temperature. Since circuit simulations require the driver's overall temperature and the LEDs' junction temperature, which determine the degradation parameters of the LED light source and the driver, the electronic and thermal simulations are coupled through both degradation models, and therefore, an iteration process among electronic and thermal simulation is required. As a result, the lumen flux depreciation as a function of time can be obtained. Generally, the useful lifetime of LED lighting products is typically given in terms of the expected operating hours until light output has depreciated to 70% of initial levels [2].

16.2.1 Degradation Modelling

16.2.1.1 LED Light Source

The exponential model is applied to describe lumen depreciation in the constant junction temperature T_j and the constant driving current I as follows [2]:

$$\Phi_{\mathrm{lm}}(t) = \Phi(I) \cdot e^{-\beta(T_j)\cdot t} \tag{16.1}$$

where t is time, Φ_{lm} is the absolute luminous flux at time t, $\Phi(I)$ is the luminous flux before aging, and the depreciation rate β follows the Arrhenius Eq. 16.5:

$$\beta(T_j) = A_\beta \cdot \mathrm{e}^{-\frac{E_{a,\beta}}{\kappa \cdot T_j}} \tag{16.2}$$

where A_β is the pre-exponential factor and $E_{a,\beta}$ is the activation energy of LED.

$\Phi(I)$ in Eq. 16.1 can be described by the following function [40]:

$$\Phi(I) = \eta(I) \cdot I \cdot V_f \tag{16.3}$$

where V_f is the forward voltage and $\eta(I)$ is the efficacy of the LED light source in current I. V_f is a function of junction temperature and current and will be introduced in the following section. The efficacy η is affected by both temperature droop (T-droop) and current droop (J-droop) [41, 42]. However, in high current status, the T-droop becomes negligible in comparison with the J-droop. Thus, η can be assumed approximately as a function of the J-droop [42]:

$$\eta = \eta_0 \cdot \frac{bn^2}{an + bn^2 + cn^3} \tag{16.4}$$

where η_0 is the basic efficacy, a and c are the linear and the third-order non-radiative recombination rates, b is the radiative recombination rate, and n is the average carrier density of LED, which is proportional to the current I; hence, the efficacy can be described the following function:

$$\eta(I) = \eta_0 \cdot \frac{B_e I}{A_e + B_e I + C_e I^2} \tag{16.5}$$

where η_0, A_e, B_e, and C_e are dependent on the properties of materials and structure of the LED.

Combined Eqs. 16.1, 16.3, and 16.5, the luminous flux in the ever-changing junction temperature $T_j(t)$ and current $I(t)$ can be described by the following function [43]:

$$\Phi_{\mathrm{lm}}(t) = \eta_0 \cdot \frac{B_e I(t)^2}{A_e + B_e I(t) + C_e I(t)^2} \cdot V_f \cdot e^{-\int_0^x \beta[T_j(x)] \cdot \mathrm{d}x} \tag{16.6}$$

The derivation of Eq. 16.6 is shown in the Appendix A. System conditions, $I(t)$, V_f, and $T_j(t)$, depend on structure and materials' properties of the lamp and circuit and can be determined by the electronic-thermal simulations. The physical characteristics of the selected LED, η_0, A_e, B_e, C_e, A_β, and $E_{a,\beta}$, are invariables and can be extracted by experiments. In this section, η_0, A_e, B_e, and C_e were determined experimentally for the selected LED, and their values are shown in Table 16.2. A_β and $E_{a,\beta}$ will be adjusted through a parametric study in Sect. 16.2.3.3.

16.2.1.2 LED Driver

Literature [33, 34] has shown that the on-state resistance of a MOSFET of an LED driver increases with aging process, leading to the degradation of output current. The study in [36] also indicates that the transistor declines during operation and brings a decreasing output current of the driver. In the present work, the degradation of the driver in terms of the output current is considered. The effective value of the output current I can be represented by the following equation:

$$I(t) = \frac{V_{\mathrm{ref}}}{R_{\mathrm{ref}}} \tag{16.7}$$

where V_{ref} is a constant reference voltage and R_{ref} is the overall current control resistance. Research in [44] has shown that the resistance of current control device degrades linearly with time. Thus, a linear degradation model for the overall current control resistance R_{ref} is assumed:

$$R_{\mathrm{ref}}(t) = R_0 \cdot [1 + A(T_D) \cdot t] \tag{16.8}$$

where R_0 is the initial resistance, T_D is the average driver temperature, and the degradation rate A follows the Arrhenius equation:

$$A(T_D) = A_0 \cdot e^{-\frac{E_{a,D}}{\kappa \cdot T_D}} \tag{16.9}$$

where A_0 is the basic degradation rate and $E_{a,D}$ is the overall activation energy of LED driver. If the driver temperature T_D changes continuously in time t, Eq. 16.8 can be deduced to an integration form, as follows:

$$R_{\text{ref}}[t, T_D(t)] = R_0 \cdot \int_0^t \{1 + A[T_D(x)] \cdot x\} \cdot \mathrm{dx} \tag{16.10}$$

where the driver temperature $T_D(t)$ is a system condition and can be determined by electronic-thermal simulations. Among the physical characteristics of the selected driver, R_0 can be determined by the initial current of the LED light source, $E_{a,D}$ and A_0, which control the driver degradation, and will be adjusted through a parametric study in Sect. 16.2.3.3.

16.2.2 Simulation Methodology

16.2.2.1 Electronic Simulations

In the present study, electronic simulations are carried out to analyze circuit behaviors of an entire LED lamp. The current, voltage, and power dissipation of each component can be calculated. The LTSPICE is selected as the electronic simulation platform. An electrolytic capacitor-free buck-boost converter, as shown in Fig. 16.1, is selected as LED driver. This type of LED driver is one of the most commonly used drivers that can achieve high efficiency, wide voltage range, and low distortion of line current in lighting applications [31]. In this section, the driver's switching frequency is 300 kHz, the input voltage range is 9–20 Vdc, the rated output current is 400 mA, the duty cycle is 25%, and the rated output power is 6.0 W. Device models in the driver, which are provided by a public database [45], have been validated and verified.

A temperature-dependent model for the LED light source is considered in circuit analysis. In this model, the performance of the LED light source can be described by the following equation [40]:

$$V_f\left[I(t), T_j(t)\right] = N \cdot \kappa \cdot T_j(t) \cdot \ln\left[\frac{I(t)}{I_s} + 1\right] + R_s \cdot I(t) \tag{16.11}$$

where N is the ideality factor, I_s is the saturation current, and R_s is the equivalent series resistance of the LED light source. Literature [46] suggests that the electronic characteristics of LEDs after seasoning is not affected by aging time but strongly affected by junction temperature T_j. Thus, the R_s, I_s, and N are considered as the

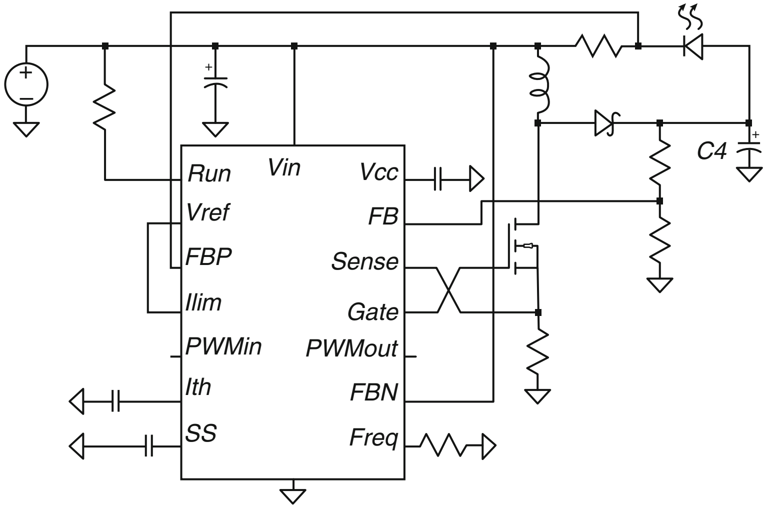

Fig. 16.1 The electrolytic capacitor-free buck-boost LED driver

functions of junction temperature T_j as following, according to literature [40, 47, 48]:

$$R_s\left[T_j(t)\right] = R_{s0} \cdot \left[1 + A_s \cdot T_j(t)\right] \tag{16.12}$$

$$I_s\left[T_j(t)\right] = I_{s0} \cdot T_j^2(t) \cdot e^{-\frac{A_I}{T_j(t)}} \tag{16.13}$$

$$N\left[T_j(t)\right] = \frac{T_j(t)}{A_N \cdot T_j(t) + B_N} \tag{16.14}$$

The power distribution of the entire circuit can be obtained by circuit simulations. The thermal power of the LED light source P_L is the difference between input power and optical power of the LED light source:

$$P_L(t) = I(t) \cdot V_f\left[I(t), T_j(t)\right] - C \cdot \Phi_{\mathrm{lm}}(t) \tag{16.15}$$

where C is the ratio of optical power and luminous flux.

The thermal power of the driver P_D is the sum of heat from all components in the driver. Thus, P_D equals to the difference between total input power and total output power of the driver:

$$P_D(t) = P_{\mathrm{in}}(t) - I(t) \cdot V_f\left[I(t), T_j(t)\right] \tag{16.16}$$

where P_{in} is the total input power.

16.2.2.2 Thermal Simulations

This chapter selects a commercial available LED light bulb as the carrier for the study. Figure 16.2 displays the lamp's structure, in which the geometrical information and material properties can refer to the literature [49–52]. In such lamps, the LED light source and driver are assembled together; thus, the heat generated by both the LED light source and the driver determine the junction temperature of the LED light source as well as the driver's temperature. As a result, system level finite element modeling is required to obtain accurate temperatures. The entire lamp operates at room temperature (298 K) with natural convection condition.

In the thermal finite element model, the driver and its potting materials as a whole are considered as a volume with a thermal conductivity of the potting material. The driver temperature, T_D, is defined as the maximum temperature of the volume. As the input of thermal simulations, the thermal power of the LED light source and the driver, P_L and P_D, are calculated by the electronic simulations. By performing the thermal simulations, T_j and T_D can be obtained which are significant to the degradations and electronic characteristics of the entire system.

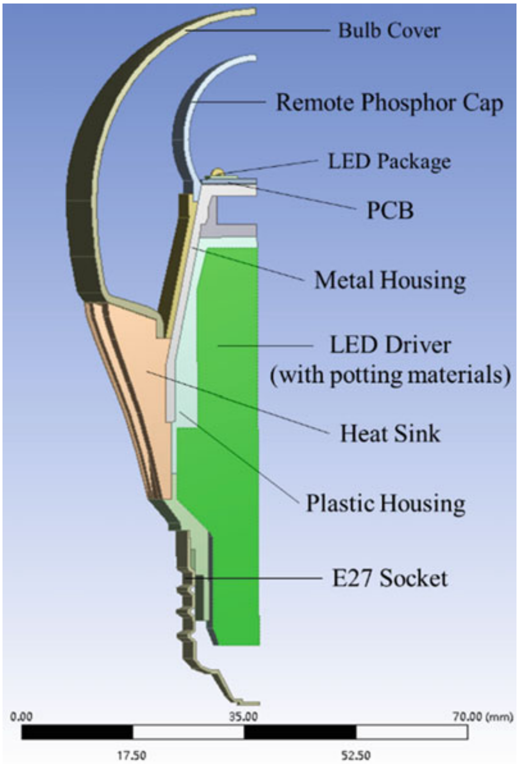

Fig. 16.2 The model of the selected (**a**) LED lamp

16.2.2.3 Simulation Methodology

Figure 16.3 illustrates the flowchart of the electronic-thermal simulation methodology in our present study. The simulation process begins with the initial guess of T_j and T_D and the LED's initial forward voltage V_f, from which the degradation models in Eqs. 16.6 and 16.10 can be applied to obtain the luminous flux Φ_{lm} and the current I. Then the electronic simulations are performed to update V_f and obtain the power dissipations by Eqs. 16.11, 16.15, and 16.16. Subsequently, the thermal simulations are performed to update T_j and T_D. Such a simulation process loop is performed iteratively until the error between values of T_j in two consecutive steps is less than 0.1 °C, as shown in Fig. 16.3. Then light output can be calculated using Eq. 16.6. Generally, the useful lifetime for LED lighting products are typically given in terms of the expected operating hours until light output has depreciated to 70% of initial levels [2]. If this threshold is not reached, the aging time t advances to a small increment Δt. Since the temperatures update T_j and T_D are not known at $t+\Delta t$, the above iteration process repeats. When time $t = t_{\mathrm{F}}$, and the Φ_{lm} has depreciated to 70% of initial value, the simulation stops, and t_{F} is considered as

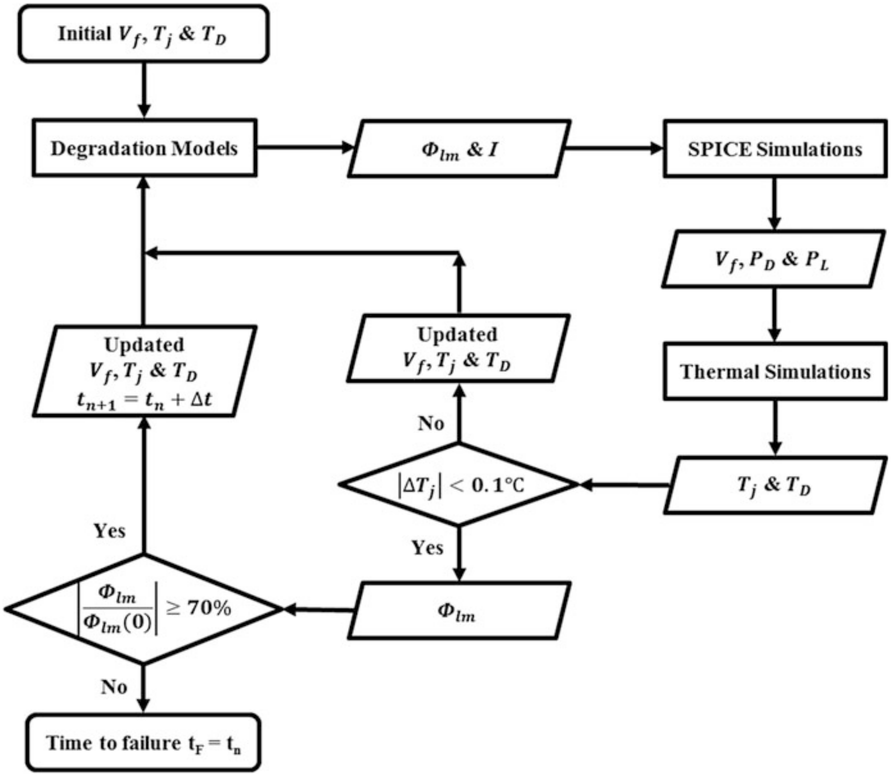

Fig. 16.3 Flowchart of the electronic-thermal simulation methodology

the lifetime of the LED system. Through the simulation iteration, the LED current, the LED junction temperature, the driver's temperature, and the luminous flux can be obtained as function of time.

16.2.3 Results and Discussions

16.2.3.1 Parameter Extraction of LED Models

The physical parameters of the lumen depreciation model and the electronic model of the LED light source, C, η_0, A_e, B_e, C_e, R_{s0}, A_s, I_{s0}, A_I, A_n, and B_n, need to be determined experimentally. Hence, selected high-power LED packages were tested in eight junction temperature levels, from 293 to 363 K. Each sample was placed on a thermal plate inside a 50 cm integrating sphere system. Then, the transient electronic and optical characteristics of each sample, including current, forward voltage, luminous flux, and efficacy, are measured at different junction temperature levels. For each junction temperature, the transient current of each sample sweeps from 200 to 350 mA. As shown in Fig. 16.4, the measured I–V characteristics were fitted by Eqs. 16.11, 16.12, 16.13, and 16.14, whereas the efficacy was fitted by Eq. 16.5 by the least square method, obtaining these physical parameters of the LED models. Table 16.1 summarizes the averaged values of the model parameters. The details of tests and parameter extractions can refer to the Literature [43].

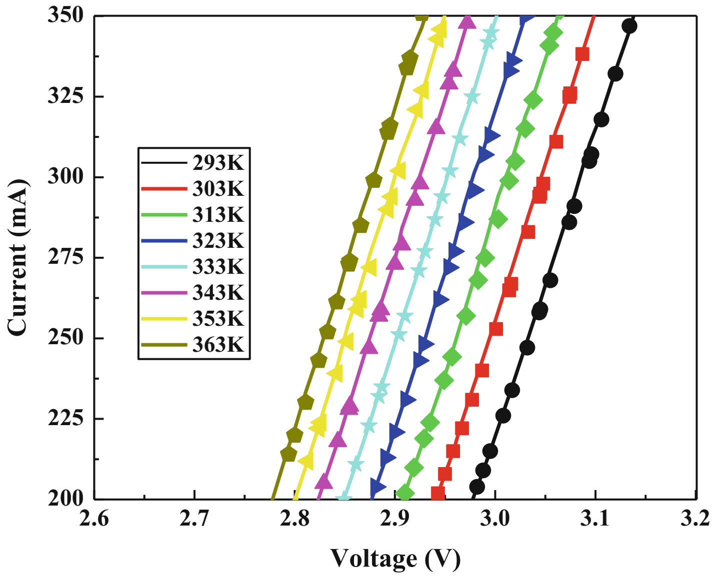

Fig. 16.4 Test results of the selected LED

Table 16.1 Physical parameters of the LED light source

R_{s0}	A_s	I_{s0}	A_I
5.914×10^{-1}	6.699×10^{-4}	4.786×10^{5}	1.274×10^{-1}
A_n	B_n	**C**	η_0
1.240	$-2.882\ 10^{2}$	4.087×10^{-3}	1.456×10^{2}
A_e	B_e	C_e	
0.999	$1.406\ 10^{3}$	2.138×10^{3}	

Table 16.2 Temperature distributions

	Predicted initial temperature (K)	Targeted temperature (K)
T_j	352	358
T_D	318	328

16.2.3.2 Lamp's Initial Temperature Distributions

It is important to know the initial temperature distributions within the lamp under operating conditions. The electronic-thermal simulations were carried out to obtain the power distributions and the ensuing initial temperature distributions. Table 16.2 lists the results of initial T_j and T_D, LED junction temperature and driver overall temperature. Table 16.2 also gives the targeted temperatures of T_j and T_D for the selected lamp. It can be seen that the predicted initial temperatures are within the design specifications. The proposed simulation method provides a useful verification tool for LED lamp design.

Due to the degradations of the LED and driver over time, both T_j and T_D will change continuously with time, which ultimately will affect the LED light output. These results will be presented and discussed in subsection 16.2.3.4.

Based on the predicted initial temperatures, the LED light source and driver can be preselected to meet the lifetime requirement. For example, LED may be selected to have 25,000 h lifetime in the predicted initial LED temperature. This means that the selected LED will have luminous flux above 70% of initial levels before 25,000 h. Similarly, the driver may also be preselected to have 25,000 h lifetime at the predicted initial driver temperature. This implies that the output current from the driver will not decrease to the certain level of the initial value (e.g., 10% of output current) before 25,000 h.

The question now is what is the lamp's ultimate lifetime in terms of luminous flux if the LED and driver's lifetimes are both 25,000 h? In the following, three scenarios are defined to study the problem.

16.2.3.3 Definition of Different Scenarios

Usually, LED's lifetime is defined at the targeted constant temperature and constant current. In the present study, as shown above, the LED is selected to have a lifetime

Table 16.3 Designed scenarios

Case	LED	Driver
Scenario 1	25,000 h lifetime at the constant initial T_j (L25K)	No degradation
Scenario 2	No degradation	25,000 h lifetime at the constant initial T_D (D25K)
Scenario 3	25,000 h lifetime at the constant initial T_j (L25K)	25,000 h lifetime at the constant initial T_D (D25K)

of 25,000 h at the initial temperature of operation, denoted as "L25K" throughout the subsequent analysis. Similarly, "D25K" indicates the 25,000 h lifetime for the selected driver at the initial temperature T_D of lamp operation. Table 16.3 lists the three scenarios to be analyzed. Scenario 1 considers LED light source degradation only with the selection of L25K LEDs. Scenario 2 considers the driver degradation only with the selection of a D25K driver. The Scenario 3 considers both of the degradations from LED and driver simultaneously. It should be noted that there are different choices of LEDs to reach L25K lifetime, with a combination of the activation energy $E_{a,\beta}$ and the pre-exponential factor A_β in Eq. 16.2. Nonetheless, unless specified, the values of $E_{a,\beta} = 0.3\text{eV}$ and $A_\beta = 2.8293 \times 10^{-1}$ are used throughout the Sect. 16.2.

16.2.3.4 Results and Discussions

LED Current

Figure 16.5 shows the relative LED current with respect to the initial value in each scenario as a function of operation time. As expected, the LED current maintains at its initial value for Scenario 1 as the driver's degradation is not considered. Since the selected driver is a constant current driver, the lumen depreciation has a negligible effect on the driver's output current. For Scenario 2 where only driver's degradation is considered, the LED current drops 10% at 25,000 h. When two degradations are considered, the LED current drops a little more, about 11% at 25,000 h.

LED Junction Temperature

Figure 16.6 shows the LED junction temperature as a function of operation time in each scenario. The LED junction temperature increases significantly in 25,000 h for Scenario 1. This is because when LED experiences the lumen depreciation, more heat is generated by the LED, leading to the temperature rise. However, the LED junction temperature decreases for Scenario 2 when the driver's degradation is considered only. This is because that driver's current degrades over time, as seen in

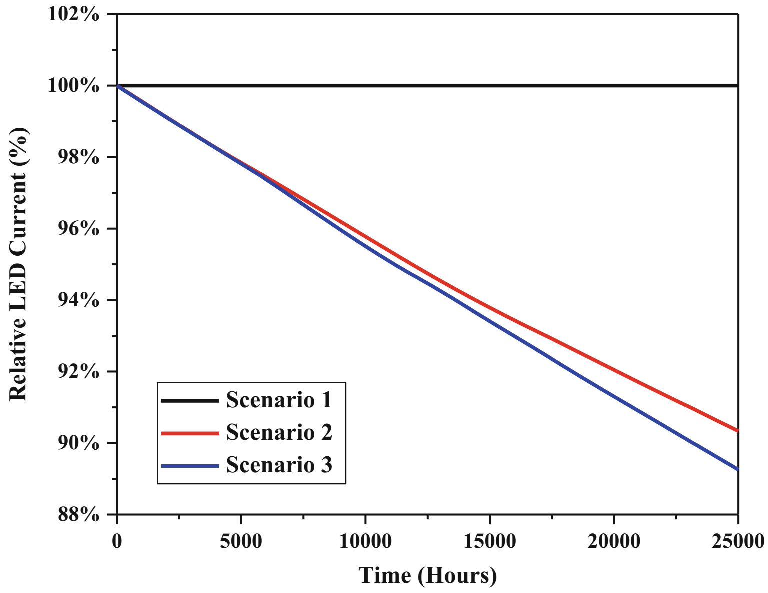

Fig. 16.5 The LED current of each scenario

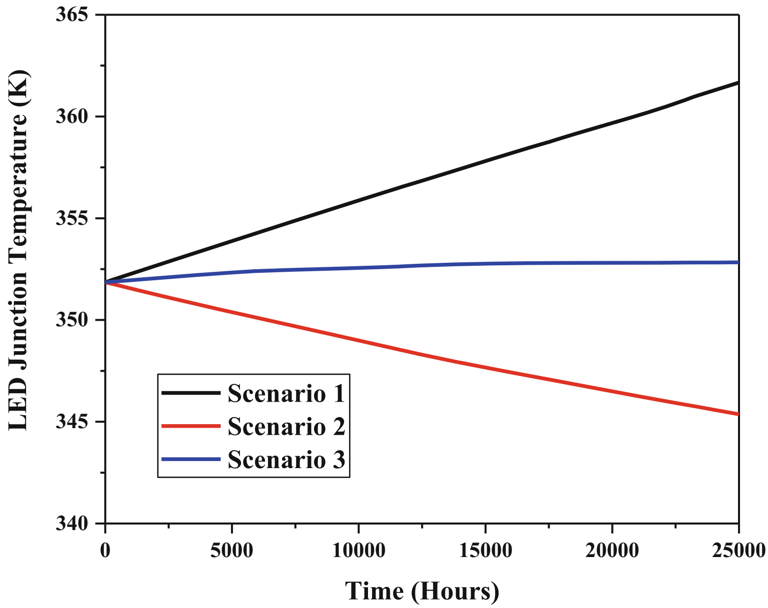

Fig. 16.6 The LED junction temperature of each scenario

Fig. 16.5; thus, less power is consumed by LEDs. It is found that the two degradations have competing effects on the junction temperatures of the LED in a lamp. As a result, Fig. 16.6 shows that LED's junction temperature does not change much for

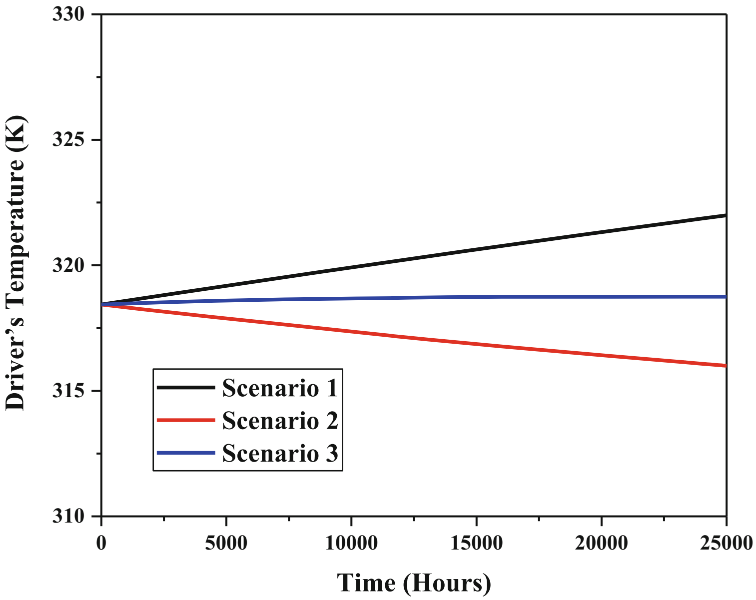

Fig. 16.7 The driver's temperature of each scenario

Scenario 3. When both degradations are considered, the LED junction temperature increases slightly initially and then decreases over time, but in a very narrow range. Overall LED temperature maintains a relatively constant value throughout 25,000 h. It should be noted that the actual LED junction temperature is not a simple superposition of Scenarios 1 and 2 but through the coupled electronic-thermal simulation.

Driver's Temperature

Figure 16.7 shows the driver's temperature as a function of operation time in each scenario. The driver's temperature increases about 3.5 K in 25,000 h for Scenario 1 and decreases about 3 K in the same time period for Scenario 2. As a result, the driver's temperature does not change much for Scenario 3. It is noted that the driver's temperature change is not as much as the LED junction temperature change for Scenarios 1 and 2.

Lumen Maintenance and Lifetime

Figure 16.8 shows the lumen maintenance of each scenario. For Scenario 1, the lumen maintenance drops to 70% in about 21,500 h. This means that even the LED is preselected as 25,000 h lifetime at the initial temperature, it's actual lifetime is

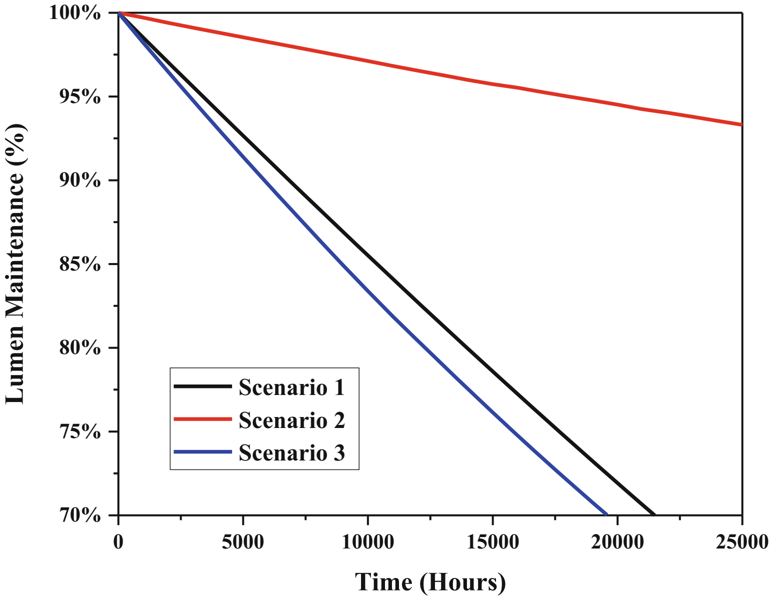

Fig. 16.8 The Lumen maintenance and for each scenario

Table 16.4 Lifetime of each combination

Combination	Lifetime
L25K D15K	18,400 h
L25K D25K	19,600 h
L25K D35K	20,100 h

reduced to 86% due to junction temperature rise. For Scenario 2, the lumen depreciation in 25,000 h is just about 7% due to the driver's degradation. In this case where LED assumes no degradation, the lumen depreciation occurs due to the reduction of both current and temperature.

For Scenario 3, the lamp's actual lifetime is about 19,600 h under the combined effect of degradations of both the LED light source and the driver, which is about 22% reduction of the initial lifetime.

The simulation results shown above illustrate only one case where the LED's lifetime (in terms of lumen depreciation) is same as the driver's lifetime (in terms of output current degradation). However, the presented methodology can be applied to any combinations of driver's and LED's lifetimes to obtain the ultimate lifetime of the lamp. Table 16.4 shows the lamp's actual lifetime for three different combinations of driver/LED lifetime selections. The D15K, D25K, and D35K represent the driver's lifetime of 25,000, 35,000, 15,000 h, respectively, while LED's lifetime remains 25,000 h (L25K). Obviously, the lamp's actual lifetime increases with the driver's lifetime but is not proportional to it. The lifetime of each combination should be differently predicted.

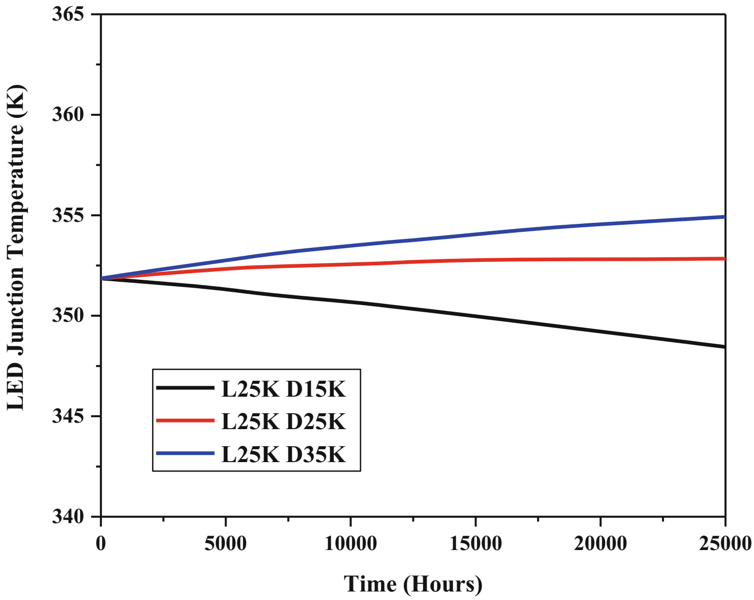

Fig. 16.9 The LED junction temperature of each combination

Figure 16.9 shows the LED junction temperature of each combination. Unlike the L25K/D25K, the LED junction temperature of the L25K/D35K case rises and the junction temperature of the L25K/D15K case falls throughout the operation time. Under effects of the interaction between degradations of the LED and the driver, these combinations have respective junction temperature curves. Thus, it is necessary to calculate the junction temperature differently by the proposed electronic-thermal simulations.

16.3 The Catastrophic Failure Under Lumen Depreciation

This section focuses on predicting the catastrophic failure of an electrolytic capacitor-free LED driver during the lumen depreciation process. The overall catastrophic failure rate of the critical components in this driver is considered as functions of temperature and current. Similar to interactions of degradations discussed in Sect. 16.2, electronic-thermal simulations are utilized to obtain the lamp's dynamic history of temperature and electrical current for two distinct modes: constant current mode (CCM) and the constant optical output (CLO) mode, respectively. A fault tree method is applied to calculate the system's MTTF, and the LED's lifetime in terms of light output can also be calculated.

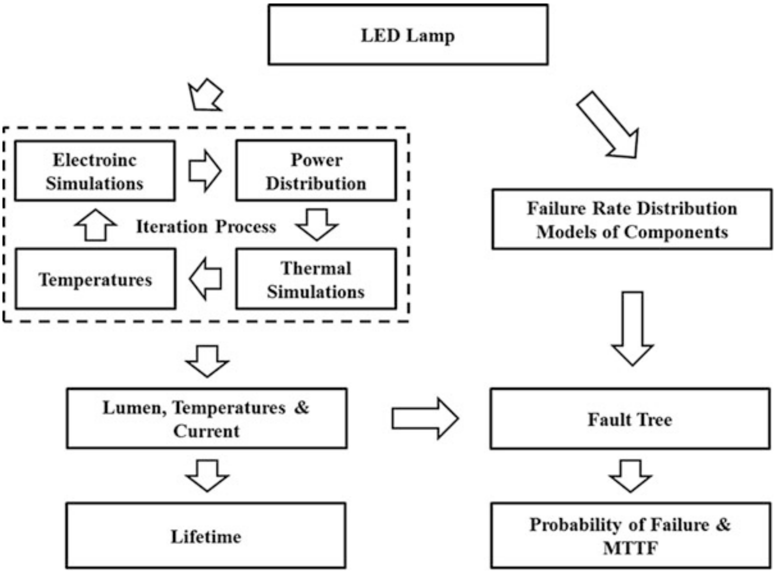

Fig. 16.10 General methodology of the proposed approach

16.3.1 General Methodology

Figure 16.10 displays the general methodology that integrates the electronic thermal simulation with the fault tree method to obtain both the LED's lifetime and driver's probability of failure and MTTF. For a given LED system, such as an LED lamp and the selected driver, electronic models are applied to obtain the power distributions of each component including LEDs. Based on the system's structure and materials, thermal simulations that combine both system-level thermal modeling and compact models are conducted. An iteration process is necessary at each operation time point to determine the state of temperature for the given system under operating condition. Details of the electronic thermal simulations can be found in the literature [3, 19]. Through the electronic thermal simulation, the junction temperature of the LED light source, current of the driver, and the lumen output can be obtained. Based on the failure rate distribution models of the critical components and the results of temperature and current, the fault tree model can be applied to obtain the driver's probability of failure and MTTF.

16.3.2 Modelling

16.3.2.1 Driver Circuit

Figure 16.11 displays the circuit of the driver. A fly-back LED driver with LC filter is selected. The LC filter can store energy as capacitors; thus, it is considered as one

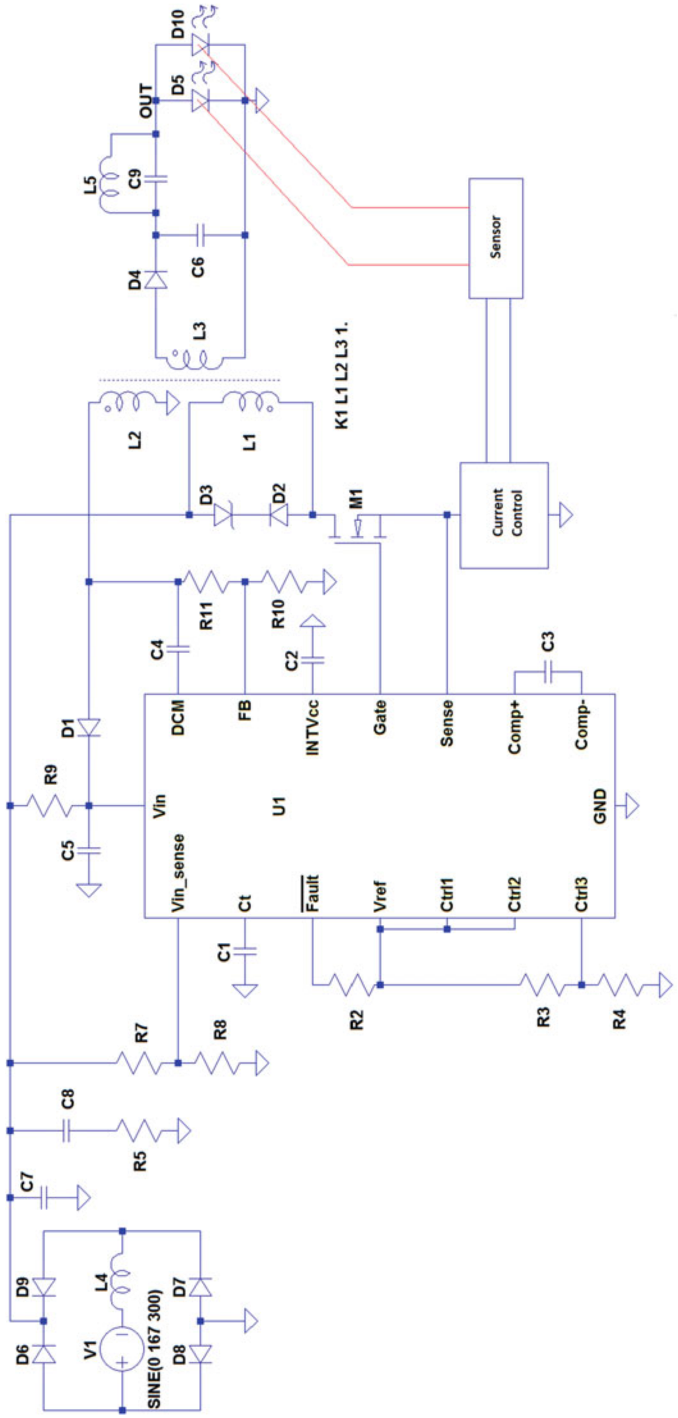

Fig. 16.11 Fly-back LED driver with LC filter

of the most cost-effective electrolytic capacitor elimination methods [28, 29]. In this circuit, the models of all components are well validated and verified by manufacturers [45]. An ideal feedback sensor and a current control unit are added, making this driver have two operation modes: the constant current mode (CCM) and the constant light output mode (CLO). In the constant current mode, the current from the driver to the LED light source remains unchanged. The current can be adjusted to achieve invariant light output in CLO mode.

16.3.2.2 Model of LED Light Source

This section uses same LED models as Sect. 16.2. Since, the CLO mode may increase the LED's junction temperature significantly. Thus, in this section, it limits the maximum junction temperature of LEDs. When its junction temperature exceeds the maximum limit T_{MAX}, the LED is supposed to be burned and give zero luminous flux. When the LED junction temperature within its limitation, the luminous flux is a function of the ever-changing junction temperature $T_j(t)$ and current $I_{\mathrm{LED}}(t)$ as discussed in Sect. 16.2. As a result, the luminous flux $\Phi_{\mathrm{lm}}(t)$ described by Eq. 16.6 can be replaced by the following function:

$$\Phi_{\mathrm{lm}}(t) = \begin{cases} \eta_0 \cdot \dfrac{B_e I_{\mathrm{LED}}(t)^2}{A_e + B_e I_{\mathrm{LED}}(t) + C_e I_{\mathrm{LED}}(t)^2} \cdot V_f \cdot e^{-\int_0^t \beta\left[T_j(x)\right] \cdot \mathrm{dx}} & \left(T_j < T_{\mathrm{MAX}}\right) \\ 0 & \left(T_j \geq T_{\mathrm{MAX}}\right) \end{cases} \tag{16.17}$$

In this section, $T_{\mathrm{MAX}} = 423$ K.

16.3.2.3 Thermal Model

Since there are several heat source, system level thermal simulations are required to obtain accurate temperatures. This section uses same thermal models of the LED lamp as Sect. 16.2. Thermal simulations in this section consist of two parts. Firstly, the finite element thermal analysis is carried out to calculate the LEDs' junction temperature T_{LED} and the driver's overall temperature T_D as Sect. 16.2. Then, the thermal compact model of each critical component in the driver is used to find their junction temperature:

$$T_{j,i} = T_D + R_{\mathrm{th},i} \cdot P_{\mathrm{th},i} \tag{16.18}$$

where $T_{j,i}$ is the junction temperature of the component, $R_{\mathrm{th},i}$ is the thermal resistance from junction to surface of the component which is usually provided by components' datasheets, and $P_{\mathrm{th},i}$ is the thermal power of the component which can be obtained by electronic simulations.

16.3.3 Fault Tree and Failure Rate Models

As a carrier of the proposed method, this section considers the catastrophic failures of the MOSFET M1 and the diode D4 in the circuit shown in Fig. 16.11. Thus, the catastrophic failure of the driver can be described by a fault tree shown in Fig. 16.12.

Assuming that the failures of the MOSFET and the diode are independent to each other, the probability density of the catastrophic failure of the LED driver can be described by the following function:

$$f_{\mathrm{Driver}}(t) = f_M(t) + f_D(t) - f_M(t) \cdot f_D(t) \tag{16.19}$$

where f_{Driver} is the failure probability density of the LED driver at time t, f_M is the failure probability density of the MOSFET, and f_D is the failure probability density of the diode.

The failure probability density of a MOSFET can be described by the inverse power law [53]:

$$f_M(t) = f_M[I_M(t), T_M(t)] = f_{M0} \cdot \left[\frac{I_M(t)}{I_{\mathrm{rated}}}\right]^p \cdot e^{-\frac{E_{a,M}}{k}\left[\frac{1}{T_M(t)} - \frac{1}{T_A}\right]} \tag{16.20}$$

where $I_M(t)$ is the average current of the MOSFET at time t, $T_M(t)$ is junction temperature of the MOSFET at time t, f_{M0} is the failure probability density of the MOSFET in rated current I_{rated} and typical ambient temperature $T_A = 298$ K, p is the current accelerated coefficient, and $E_{a,M}$ is the activation energy of the MOSFET.

Similar to the MOSFET, the failure probability density of a diode can be described by the [53]:

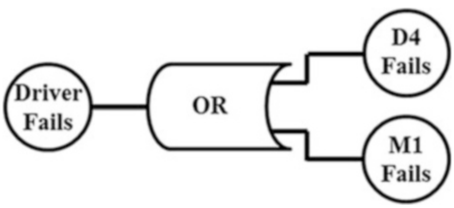

Fig. 16.12 The fault tree of the LED driver

$$f_D(t) = f_D[T_{\mathrm{Di}}(t)] = f_{D0} \cdot \mathrm{e}^{-\frac{E_{a,D}}{k}\left[\frac{1}{T_{\mathrm{Di}}(t)} - \frac{1}{T_A}\right]} \tag{16.21}$$

where f_D is the failure probability density of the diode, $T_{\mathrm{Di}}(t)$ is junction temperature of the diode at time t, f_{D0} is the rated failure probability density of the diode in typical ambient temperature $T_A = 298$ K, and $E_{a,D}$ is the activation energy of the diode.

The conditions $I_M(t)$, $T_M(t)$, and $T_{\mathrm{Di}}(t)$ at each operation time point can be obtained by the electronic-thermal simulations, and thus, the failure probability densities f_M, f_D, and f_{Driver} at each time point can be calculated by Eqs. 16.8, 16.9, and 16.10. Then, the mean time to failure (MTTF) of the LED driver can be calculated by the following equation:

$$\mathrm{MTTF} = t_{\mathrm{MAX}} / \int_0^{t_{\mathrm{MAX}}} f_{\mathrm{driver}}(t) \cdot \mathrm{dt} \tag{16.22}$$

where t_{MAX} is the total operation duration.

16.3.4 Case Studies and Results

16.3.4.1 Selection of LED and Driver

To estimate the actual lifetime and the MTTF of the investigated LED lamp, the LED light source is preselected with the activation energy and pre-factor of $E_{a,\beta} = 0.3$eV and $A_\beta = 0.2829$, according to our previous test results [43]. According to the electronic thermal simulation at the initial state during operation, the LED's junction temperature in the lamp is about 351 K. Based on the parameters defined above, the LED's lifetime is 25,000 h in terms of lumen depreciation at the constant 351 K with a current of 400 mA, by Eqs. 16.1 and 16.2. It means that the lumen maintenance is above 70% of its initial value in 25,000 h if the LED temperature maintains at 351 K, and it's current of 400 mA does not change during operation.

For LED driver, the empirical values of model parameters for the MOSFET M1 and diode D4 in the circuit are selected as from the literature [54] p of 2.0 and as $E_{a,M}$ and $E_{a,D}$ of 0.7 eV, respectively. Without any lumen degradation, the driver's average temperature in the lamp is defined as the initial driver temperature $T_D(0)$, and the junction temperatures of M1 and D4 in $T_D(0)$ are called initial junction temperatures of M1 and D4, $T_M(0)$, and $T_{\mathrm{Di}}(0)$. According to simulation results, the values of $T_D(0)$, $T_M(0)$, and $T_{\mathrm{Di}}(0)$ are about 342 K, 363 K, and 350 K respectively. To ensure the MTTF of the driver before lumen depreciation equals to the lifetime, it supposes $f_{M0} = 2.31 \times 10^{-7}$, $f_{D0} = 1.54 \times 10^{-7}$. As a result, the MTTF of M1 in $T_M(0)$ is about 32,000 h; the MTTF of D4 in $T_{\mathrm{Di}}(0)$ is about 109,000 h, according to Eqs. 16.9 and 16.10. This means that the driver's MTTF is about 25,000 h in $T_D(0)$, and MOEFET's current I_M does not change during operation, according to the fault tree model to used.

Both of the lifetime and MTTF are 25,000 h without the lumen degradation. However, since the junction temperature in the lamp during operation will change over time, to be shown in details later, the actual LED's lifetime will be different from the preselected lifetime. Since values of T_D, $T_M(0)$, and $T_{\mathrm{Di}}(0)$ change over time during operation, and the failure rate of the M1 also depends on the current I_M, the actual MTTF of the driver will also different from the preselected MTTF. The details of the results will be discussed below.

16.3.4.2 Results and Discussions

Constant Light Output (CLO) Mode

Figure 16.13 displays the LED current curve at the CLO mode. The LED's current increases exponentially, e.g., from the initial 400 to 730 mA in 14,000 h. Such an increase in current mainly compensates the luminous flux degradation of the LED to maintain the constant light output.

Figure 16.14 displays the LED junction temperature as a function of time. Due to the increased current, the LED's temperature increases greatly. At 14,000 h, the junction temperature of the LED light source increases about 75 K and exceeds 423 K.

Figure 16.15 shows the history of the junction temperatures of M1 and D4 at the CLO mode. In 14,000 h, the junction temperatures of M1 increases from 363 to 429 K, and the junction temperatures of D4 rises from 350 to 408 K.

Figure 16.16 shows the cumulative failure rate of M1 in different conditions of the CLO mode. In the constant temperature and current of the M1, the cumulative failure rate is about 43% at 14,000 h. If only considers increasing of M1's junction temperature, the failure rate accumulates to 100% around 12,000 h. If only considers M1's current increasing, the cumulative failure rate is about 86% at 14,000 h. If considers both of junction temperature and current of M1 in CLO mode, the failure rate of M1 accumulates to 100% in about 10,000 h. The failure rate of M1 is increased greatly in the junction temperature and current of M1. Compare with the current, the increased junction temperature has larger effects on the failure rate, due to the high activation energy.

Figure 16.17 displays cumulative failure rate of the driver in different conditions of CLO mode. In the ever-increasing temperature and current obtained by proposed models, the failure rate of the driver accumulates to 100% in about 9,300 h. In the constant temperature and current, the failure rate accumulates about 56% linearly in 14,000 h. As discussed above, failure rates of driver's components are greatly increased by driver's temperature and M1's current. Thus, the driver in CLO mode has a shorter MTTF than in constant conditions.

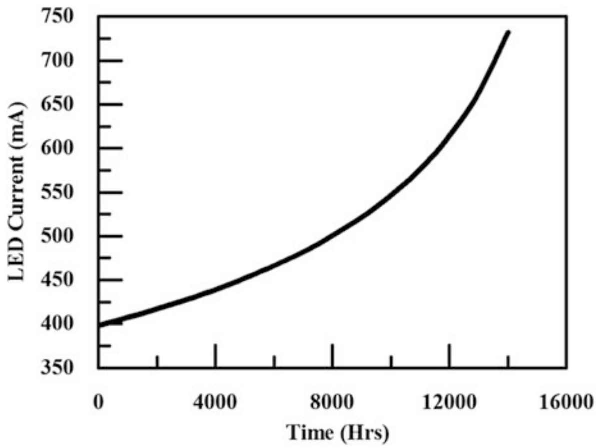

Fig. 16.13 The LED current curve of the CLO mode

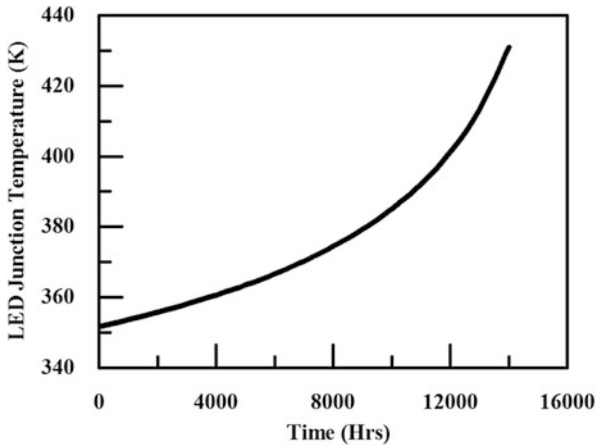

Fig. 16.14 The LED junction temperature of the CLO mode

Constant Current Mode (CCM)

Figure 16.18 displays the LED junction temperature in CCM mode. After 25,000 h, the junction temperature of the LED increases about 10 K. As the degradation process of the LED light source, more thermal power is generated, leading temperature increasing of the entire lamp. Although the increment is less than the CLO mode, the increased LED junction temperature still have a significant impact on the lamp's lifetime.

Figure 16.19 displays the normalized luminous flux of CCM mode. The lifetime of the LED lamp in this mode is around 21,500 h. The elevated junction temperature accelerates the degradation of the LED light source. Thus, the lifetime in CCM is about 14% shorter than in the constant temperature and current.

Figure 16.20 shows the history of the junction temperatures of M1 and D4 at the CCM mode. The junction temperature of M1 increases from 363 to 366 K, and D4's

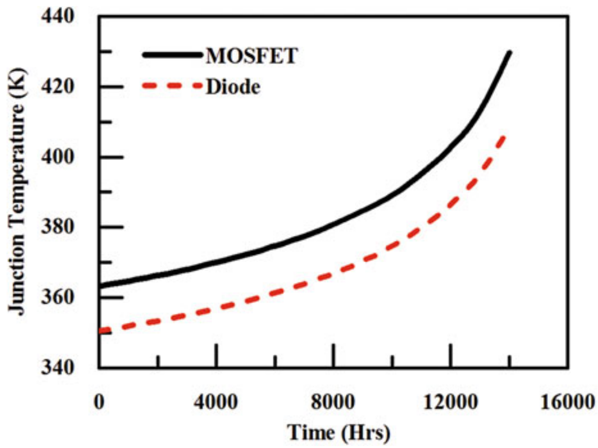

Fig. 16.15 The junction temperature of M1 and D4 of the CLO mode

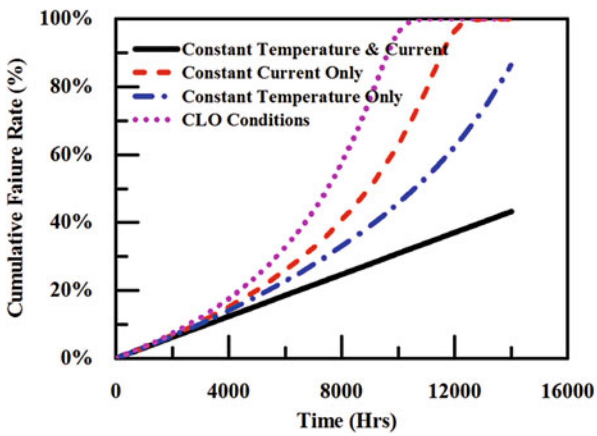

Fig. 16.16 Cumulative failure rates of M1 in the CLO mode

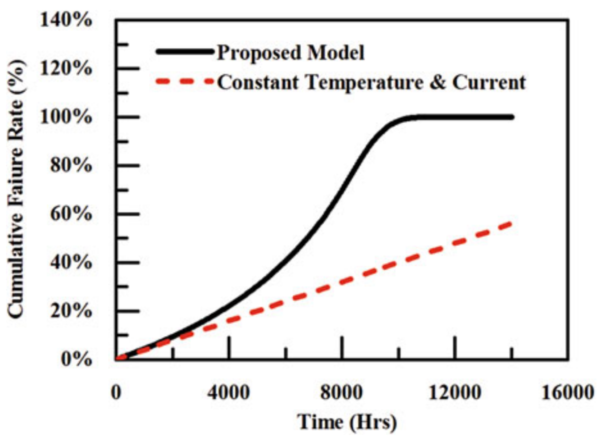

Fig. 16.17 Cumulative failure rates of the driver in CLO mode

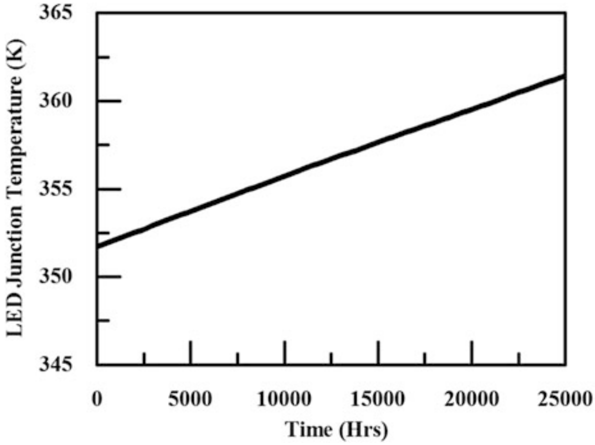

Fig. 16.18 The LED junction temperature of the CCM mode

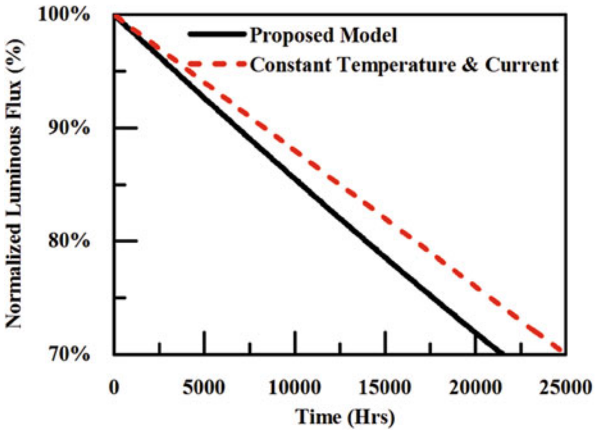

Fig. 16.19 Normalized luminous flux of the CCM mode

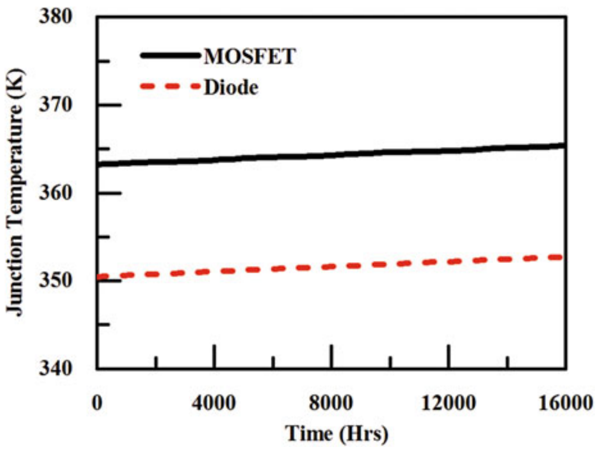

Fig. 16.20 The junction temperatures of M1 and D4 in the CCM mode

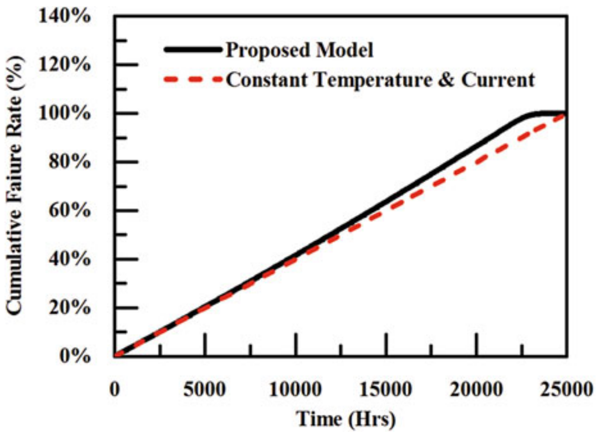

Fig. 16.21 Cumulative failure rates of the driver in the CCM mode

Table 16.5 Lists lifetimes, MTTFs, and temperatures of each mode

Case	Lifetime (H)	T_j (K)	MTTF (H)	T_D (K)
Initial status	25,000	351	25,000	342
CLO	14,000	Varying	9,300	Varying
CCM	21,500	Varying	22,900	Varying

junction temperature rises from 350 to 354 K in 25,000 h. Compared with the CLO mode, the junction temperature of M1 and D4 increases slightly.

Figure 16.21 displays cumulative failure rate of the driver in different conditions of CCM mode. In the ever-increasing temperature and current obtained by proposed models, the failure rate of the driver accumulates to 100% in about 22,900 h. In the constant temperature and current, the cumulative failure rate is about 100% at 25,000 h. As discussed above, failure rates of driver's components are slightly increased by driver's temperature. Thus, the driver in CCM mode has a little shorter MTTF than in constant conditions (Table 16.5).

In CLO mode, the lifetime is about 14,000 h since the LED junction temperature exceeds its maximum value, and the MTTF is about 9,300 h. The light output compensation brings the increased current and temperatures and, thus, a shorter lifetime and MTTF. Thus, the constant light output mode eliminates lumen depreciation at the expense of the reliability of the LED lamp. Such technologies are not suitable to improve the reliability of LED lamps. Due to the higher activation energy of the driver, the MTTF is more temperature sensitive than the lifetime. The MTTF becomes much shorter than the lifetime, and the catastrophic failure may occur before the lumen depreciation. In reliability optimization, it should put a priority on the catastrophic failure of the driver.

In CCM mode, the lifetime is about 21,500 h, and the MTTF is about 22,900 h. As the discussion above, the ever-increasing LED junction temperature accelerates the degradation process of the LED light source and brings high failure rate of the driver. Moreover, the lifetime and the MTTF in this mode are comparable. It means that both of the catastrophic failure and the lumen depreciation may occur. In reliability optimization, both of these two failure modes should be considered.

16.4 Conclusions

Section 16.2 investigates the impact of the interaction between the degradations of the LED and driver on the lifetime of an integrated LED lamp. The electronic-thermal simulation was carried out to obtain performance of the LED. Three scenarios were simulated first:

- Scenario 1 considers the LED light source degradation only, with the selection of 25,000 h LED's lifetime. In this case, LED current stays almost at its initial value due to the non-degradation driver applied. However, the LED junction temperature and the driver's temperature increase over time. As a result, the lamp's lifetime is reduced to 21,500 h, about 86% of the targeted lifetime.
- Scenario 2 considers the driver's degradation only, with a selection of 25,000 h lifetime of driver in terms of output current. Since LED's degradation is not take into consideration in this case, the LED's junction temperature and the driver's temperature decrease over operation time, as less electric current is applied. As a result, the lumen output is depreciated at only 7% in about 25,000 h. It implies that when the driver's lifetime is comparable to the LED's lifetime, the LED's degradation must be taken into considerations.
- Scenario 3 investigates the ultimate lifetime of the LED lamp when both degradations from LED and driver simultaneously occur. It has been found that the LED's junction temperature and the driver's temperature do not change much in 25,000 h. However, the lamp's lifetime in terms of lumen output has been reduced to 19,600 h.

Furthermore, the different combinations of driver/LED lifetime selections were studied, with the driver's lifetime as 25,000, 35,000, 15,000 h, respectively, while LED's lifetime remains 25,000 h. It has been found that the lifetime and the LED junction temperature of each combination need to be predicted case by case by the electronic-thermal simulations.

Section 16.3 focuses on predicting the catastrophic failure of an electrolytic capacitor-free LED driver during the lumen depreciation process. A commercial LED bulb and a fly-back converter with an LC filter are used in the present study. Electronic-thermal simulations are utilized to obtain the lamp's dynamic history of temperature and electrical current for two distinct modes: constant current mode (CCM) and the constant optical output (CLO) mode, respectively. A fault tree method is applied to calculate the system's MTTF, and the LED's lifetime also is calculated.

- The CLO mode increases exponentially the LED's current to maintain the constant light output. As a result, junction temperatures of LEDs, MOSFET, and diode rise about 75 K, 50 K, and 50 K, respectively. As a result, the lifetime decreases to 14,000 h, and the MTTF drops about 9870 h. Thus, the constant light output mode eliminates lumen depreciation at the expense of the reliability of the LED lamp. Such technologies are not suitable to improve the reliability of LED lamps. Compare with current of MOSFET, the increased junction temperature has larger effects on the failure rate. The MOSFET contributes more to the driver's failure rate than the diode. Since the MTTF is shorter than the lifetime, the catastrophic failure of the driver may occur before the lumen depreciation. In reliability optimization, it should put a priority on the catastrophic failure of the driver.

- For the CCM mode, the current keeps unchanged; junction temperatures of the LED, the MOSFET, and the diode rise about 10 K, 4 K, and 4 K respectively, leading the lifetime drops to about 21,500 h; and the MTTF drops to about 22,600 h. Similar to the CLO mode, MOSFET also contributes more to the driver's failure rate than the diode. Since the lifetime and the MTTF in this mode are comparable, both of the catastrophic failure and the lumen depreciation may occur. In reliability optimization, both of these two failure modes should be considered.

From abovementioned results and discussions, it is concluded that it is necessary to apply the electronic-thermal simulations to predict the reliability of LED lamps when driver's lifetime is comparable to the LED's lifetime. This chapter presents a methodology to accurately predict the ultimate lamp's lifetime. Such a methodology will be very useful in designing LED product by selecting different drivers and LED light sources.

References

1. J. Fan, K.C. Yung, M. Pecht, Prognostics of lumen maintenance for high power white light emitting diodes using a nonlinear filter-based approach. Reliab. Eng. Syst. Saf. **123**, 63–72 (2014)
2. C. Qian, X.J. Fan, J. Fan, C.A. Yuan, G.Q. Zhang, An accelerated test method of luminous flux depreciation for LED luminaires and lamps. Reliab. Eng. Syst. Saf. **147**, 84–92 (2015)
3. B. Sun, X.J. Fan, C. Qian, G.Q. Zhang, PoF-simulation-assisted reliability prediction for electrolytic capacitor in LED drivers. IEEE Trans. Ind. Electron., in press **63**, 6726–6735 (2016)
4. B. Sun, X. J. Fan, C. A. Yuan, C. Qian, G. Q. Zhang, A degradation model of aluminum electrolytic capacitors for LED drivers, in *2015 16th International Conference on Thermal, Mechanical and Multi-Physics Simulation and Experiments in Microelectronics and Microsystems (EuroSimE),* (2015), pp. 1–4
5. S. Koh, C. Yuan, B. Sun, B. Li, X. J. Fan, G. Q. Zhang, Product level accelerated lifetime test for indoor LED luminaires, in *2013 14th International Conference on Thermal, Mechanical and Multi-Physics Simulation and Experiments in Microelectronics and Microsystems (EuroSimE)*, (2013), pp. 1–6

6. J. Huang, S.W. Koh, D. Yang, X. Li, X.J. Fan, G.Q. Zhang, *Degradation Mechanisms of Mid-power White-light LEDs under High Temperature-Humidity Conditions*. IEEE Trans. Device Mat. Reliab. **15**, 1–1 (2015)
7. J. Huang, D.S. Golubović, S.W. Koh, D. Yang, X. Li, X.J. Fan, G.Q. Zhang, Rapid degradation of mid-power white-light LEDs in saturated moisture conditions. IEEE Trans. Device Mater. Reliab. **15**, 478–485 (2015)
8. G. Lu, W.D. van Driel, X.J. Fan, M.Y. Mehr, J. Fan, K. Jansen, G.Q. Zhang, Degradation of microcellular PET reflective materials used in LED-based products. Opt. Mater. **49**, 79–84 (2015)
9. G. Lu, M.Y. Mehr, W. van Driel, X.J. Fan, J. Fan, K. Jansen, G.Q. Zhang, Color shift investigations for LED secondary optical designs: comparison between BPA-PC and PMMA. Opt. Mater. **45**, 37–41 (2015)
10. J. Fan, C. Qian, K.C. Yung, X.J. Fan, G.Q. Zhang, M. Pecht, Optimal design of life testing for high-brightness white LEDs using the six sigma DMAIC approach. IEEE Trans. Device Mater. Reliab. **15**, 576–587 (2015)
11. R. Pinto, M.R. Cosetin, A. Campos, M.A. Dalla Costa, R.N. do Prado, Compact emergency lamp using power LEDs. IEEE Trans. Ind. Electron. **59**, 1728–1738 (2012)
12. S.R. Hui, S.N. Li, X.H. Tao, W. Chen, W. Ng, A novel passive offline LED driver with long lifetime. IEEE Trans. Power Electron. **25**, 2665–2672 (2010)
13. D.G. Lamar, M. Arias, A. Rodriguez, A. Fernandez, M.M. Hernando, J. Sebastián, Design-oriented analysis and performance evaluation of a low-cost high-brightness LED driver based on flyback power factor corrector. IEEE Trans. Ind. Electron. **60**, 2614–2626 (2013)
14. X. Qu, S.C. Wong, C.K. Tse, Resonance-assisted buck converter for offline driving of power LED replacement lamps. IEEE Trans. Power Electron. **26**, 532–540 (2011)
15. X. Wu, J. Yang, J. Zhang, Z. Qian, Variable on-time (VOT)-controlled critical conduction mode buck PFC converter for high-input AC/DC HB-LED lighting applications. IEEE Trans. Power Electron. **27**, 4530–4539 (2012)
16. P.S. Almeida, D. Camponogara, M. Dalla Costa, H. Braga, J.M. Alonso, Matching LED and driver life spans: a review of different techniques. IEEE Ind. Electron. Mag. **9**, 36–47 (2015)
17. C. Branas, F.J. Azcondo, J.M. Alonso, Solid-state lighting: a system review. IEEE Ind. Electron. Mag. **7**, 6–14 (2013)
18. J.M. Alonso, J. Viña, D.G. Vaquero, G. Martínez, R. Osorio, Analysis and design of the integrated double buck–boost converter as a high-power-factor driver for power-LED lamps. IEEE Trans. Ind. Electron. **59**, 1689–1697 (2012)
19. B. Sun, X. J. Fan, W. D. van Driel, H. Ye, J. Fan, C. Qian, G. Q. Zhang, *A Novel Lifetime Prediction for Integrated LED Lamps by Electronic-Thermal Simulation*, IEEE Transactions on Industrial Electronics, Submitted 2016
20. P. S. Almeida, G. M. Soares, D. P. Pinto, H. A. Braga, Integrated SEPIC buck-boost converter as an off-line LED driver without electrolytic capacitors, in *IECON 2012-38th Annual Conference of IEEE Industrial Electronics Society*, (2012), pp. 4551–4556
21. H. Ma, J.S. Lai, Q. Feng, W. Yu, C. Zheng, Z. Zhao, A novel valley-fill SEPIC-derived power supply without electrolytic capacitor for LED lighting application. IEEE Trans. Power Electron. **27**, 3057–3071 (2012)
22. Z. Bo, Y. Xu, X. Ming, C. Qiaoliang, W. Zhaoan, Design of boost-flyback single-sage PFC converter for LED power supply without electrolytic capacitor for energy-storage, in . *2009 I. E. 6th International Power Electronics and Motion Control Conference, IPEMC'09*, (2009), pp. 1668–1671
23. H. Ma, W. Yu, C. Zheng, J. S. Lai, Q. Feng, B. Y. Chen, A universal-input high-power-factor PFC pre-regulator without electrolytic capacitor for PWM dimming LED lighting application, in *2011 I.E. Energy Conversion Congress and Exposition (ECCE)*, (2011), pp. 2288–2295
24. D. Camponogara, D. Ribeiro Vargas, M. Dalla Costa, J.M. Alonso, J. Garcia, T. Marchesan, Capacitance reduction with an optimized converter connection applied to LED drivers. Ind. Electron. IEEE Trans. **62**, 184–192 (2015)

25. C. Wong, Y. Lai, K. Loo, C. K. Tse, Elimination of electrolytic capacitor in LED power supplies by two-phase driving approach, in *2014 16th European Conference on Power Electronics and Applications* (*EPE'14-ECCE Europe*), (2014), pp. 1–9
26. K.W. Lee, Y.H. Hsieh, T.J. Liang, A current ripple cancellation circuit for electrolytic capacitor-less AC-DC LED driver, in *2013 Twenty-Eighth Annual IEEE Applied Power Electronics Conference and Exposition (APEC)*, (2013), pp. 1058–1061
27. L. Gu, X. Ruan, M. Xu, K. Yao, Means of eliminating electrolytic capacitor in AC/DC power supplies for LED lightings. IEEE Trans. Power Electron. **24**, 1399–1408 (2009)
28. B. Wang, X. Ruan, K. Yao, M. Xu, A method of reducing the peak-to-average ratio of LED current for electrolytic capacitor-less AC–DC drivers. IEEE Trans. Power Electron. **25**, 592–601 (2010)
29. X. Ruan, B. Wang, K. Yao, S. Wang, Optimum injected current harmonics to minimize peak-to-average ratio of LED current for electrolytic capacitor-less AC–DC drivers. IEEE Trans. Power Electron. **26**, 1820–1825 (2011)
30. S. Dietrich, S. Strache, R. Wunderlich, S. Heinen, Get the LED out: experimental validation of a capacitor-free single-inductor, multiple-output LED driver topology. Industrial Electronics Magazine, IEEE **9**, 24–35 (2015)
31. P. Fang, Y. F. Liu, An electrolytic capacitor-free single stage Buck-Boost LED driver and its integrated solution, in *2014 Twenty-Ninth Annual IEEE Applied Power Electronics Conference and Exposition (APEC)*, (2014), pp. 1394–1401
32. J.C. Lam, P.K. Jain, A high power factor, electrolytic capacitor-less AC-input LED driver topology with high frequency pulsating output current. IEEE Trans. Power Electron. **30**, 943–955 (2015)
33. S. Lan, C.M. Tan, K. Wu, Reliability study of LED driver–a case study of black box testing. Microelectron. Reliab. **52**, 1940–1944 (2012)
34. S. Lan, C.M. Tan, K. Wu, Methodology of reliability enhancement for high power LED driver. Microelectron. Reliab. **54**, 1150–1159 (2014)
35. D. Ang, C. Ling, On the time-dependent degradation of LDD n-MOSFETs under hot-carrier stress. Microelectron. Reliab. **39**, 1311–1322 (1999)
36. X. Shao, *Research on Reliability Assessment Method of The LED Driver Power Supply* (Master of Engineering, School of Electrical Engineering, Harbin Institute of Technology, Harbin, 2012)
37. Z.Y. Zhou Yue-ge, L. Xiang, Z. Guofu, Performance reliability assessment of LED drivers for lighting. Electri c Machines and Control **18**, 2014.09 (2014)
38. R. Wu, F. Blaabjerg, H. Wang, M. Liserre, Overview of catastrophic failures of freewheeling diodes in power electronic circuits. Microelectron. Reliab. **53**, 1788–1792 (2013)
39. Constant Light Output (CLO)., Available: http://www.lightingproducts.philips.com/our-brands/philips-controls/constant-light-output-clo.html (2014)
40. E.F. Schubert, T. Gessmann, J.K. Kim, *Light Emitting Diodes* (Wiley Online Library, Hoboken, 2005)
41. D.S. Meyaard, Q. Shan, J. Cho, E.F. Schubert, S.-H. Han, M.-H. Kim, C. Sone, S.J. Oh, J.K. Kim, Temperature dependent efficiency droop in GaInN light-emitting diodes with different current densities. Appl. Phys. Lett. **100**, 081106 (2012)
42. J. Piprek, Efficiency droop in nitride-based light-emitting diodes. Phys. Status Solidi A **207**, 2217–2225 (2010)
43. B. Sun, X. J. Fan, W. V. Driel, T. Michel, J. Zhou, G. Q. Zhang, Lumen decay prediction in LED lamps, *Presented at the IEEE International Conference on Thermal, Mechanical and Multi-Physics Simulation and Experiments in Microelectronics and Microsystems, Montpellier*, 2016
44. S. Tarashioon, W. van Driel, G.Q. Zhang, Multi-physics reliability simulation for solid state lighting drivers. Microelectron. Reliab. **54**, 1212–1222 (2014)
45. Linear Technology Corporation., LTwiki. Available: http://ltwiki.org/?title=Main_Page (2014)

46. B. Hamon, B. Bataillou, A. Gasse, G. Feuillet, N-contacts degradation analysis of white flip chip LEDs during reliability tests, in *2014 I.E. International Reliability Physics Symposium*, (2014), pp. FA. 1.1–FA. 1.6
47. H.T. Chen, S.-C. Tan, S. Hui, Color variation reduction of GaN-based white light-emitting diodes via peak-wavelength stabilization. Power Electron. IEEE Trans. **29**, 3709–3719 (2014)
48. M. Hudait, S. Krupanidhi, Doping dependence of the barrier height and ideality factor of Au/n-GaAs Schottky diodes at low temperatures. Phys. B **307**, 125–137 (2001)
49. X. Perpina, R. Werkhoven, M. Vellvehi, X. Jorda, J. Kunen, J. Jakovenk, P. Bancken, P. Bolt, LED driver thermal design considerations for solid-state lighting technologies, in *2012 13th International Conference on Thermal, Mechanical and Multi-Physics Simulation and Experiments in Microelectronics and Microsystems (EuroSimE)*, 2012, pp. 1/5–5/5
50. Y. Huaiyu, K.S. Wee, W. Jia, H.W. Van Zeijl, Dynamic thermal simulation of high brightness LEDs with unsteady driver power output, in *2012 13th International Conference on Thermal, Mechanical and Multi-Physics Simulation and Experiments in Microelectronics and Microsystems (EuroSimE)*, 2012, pp. 1/5–5/5
51. J. Jakovenko, R. Werkhoven, J. Formanek, J. Kunen, Thermal simulation and validation of 8W LED Lamp, in *2011 12th International Conference on Thermal, Mechanical and Multi-Physics Simulation and Experiments in Microelectronics and Microsystems (EuroSimE)*, 2011, pp. 1/4–4/4
52. J. Jakovenko, J. Formánek, V. Janíček, M. Husák, R. Werkhoven, High power solid state retrofit lamp thermal characterization and modeling. Radioengineering **21**, 231–238 (2012)
53. T. Santini, S. Morand, M. Fouladirad, L.V. Phung, F. Miller, B. Foucher, A. Grall, B. Allard, Accelerated degradation data of SiC MOSFETs for lifetime and remaining useful life assessment. Microelectron. Reliab. **54**, 1718–1723 (2014)
54. M.S. Handbook, *MIL-HDBK-217F: Reliability Prediction of Electronic Equipment* (US Department of Defense, Washington, DC, 1995)